OPEN ACCESS Freely available online

PLOS ONE

Phosphorylation of Mutant Huntingtin at Serine 116 Modulates Neuronal Toxicity

Erin E. Watkin[1☯], Nicolas Arbez[1☯], Elaine Waldron-Roby[1], Robert O'Meally[2], Tamara Ratovitski[1], Robert N. Cole[2], Christopher A. Ross[1,3]*

1 Division of Neurobiology, Department of Psychiatry, Johns Hopkins University School of Medicine, Baltimore, Maryland, United States of America, **2** Mass Spectrometry and Proteomics Facility, Johns Hopkins University School of Medicine, Baltimore, Maryland, United States of America, **3** Departments of Neurology, Pharmacology and Neuroscience and Program in Cellular and Molecular Medicine, Johns Hopkins University School of Medicine, Baltimore, Maryland, United States of America

Abstract

Phosphorylation has been shown to have a significant impact on expanded huntingtin-mediated cellular toxicity. Several phosphorylation sites have been identified on the huntingtin (Htt) protein. To find new potential therapeutic targets for Huntington's Disease (HD), we used mass spectrometry to identify novel phosphorylation sites on N-terminal Htt, expressed in HEK293 cells. Using site-directed mutagenesis we introduced alterations of phosphorylation sites in a N586 Htt construct containing 82 polyglutamine repeats. The effects of these alterations on expanded Htt toxicity were evaluated in primary neurons using a nuclear condensation assay and a direct time-lapse imaging of neuronal death. As a result of these studies, we identified several novel phosphorylation sites, validated several known sites, and discovered one phospho-null alteration, S116A, that had a protective effect against expanded polyglutamine-mediated cellular toxicity. The results suggest that S116 is a potential therapeutic target, and indicate that our screening method is useful for identifying candidate phosphorylation sites.

Citation: Watkin EE, Arbez N, Waldron-Roby E, O'Meally R, Ratovitski T, et al. (2014) Phosphorylation of Mutant Huntingtin at Serine 116 Modulates Neuronal Toxicity. PLoS ONE 9(2): e88284. doi:10.1371/journal.pone.0088284

Editor: David R. Borchelt, University of Florida, United States of America

Received November 25, 2013; **Accepted** January 8, 2014; **Published** February 5, 2014

Copyright: © 2014 Watkin et al. This is an open-access article distributed under the terms of the Creative Commons Attribution License, which permits unrestricted use, distribution, and reproduction in any medium, provided the original author and source are credited.

Funding: This research was supported by NINDS grant NS16375 (http://www.ninds.nih.gov/). The funders had no role in study design, data collection and analysis, decision to publish, or preparation of the manuscript.

Competing Interests: The authors have declared that no competing interests exist.

* E-mail: caross@jhu.edu

☯ These authors contributed equally to this work.

Introduction

Huntington's disease (HD) is a fatal progressive neurodegenerative disorder involving movement, cognitive and emotional symptoms, with no current neuroprotective therapy [1–10]. The striatum is the main structure of the brain affected by the neurodegeneration, but some is also notable in the cortex and other brain regions, especially in early onset cases or late stage disease [11–14]. HD is caused by a CAG triplet repeat expansion in the *Huntingtin* gene on chromosome 4 coding for a polyglutamine repeat expansion in the Huntingtin protein (Htt) [15]. There is a correlation between repeat length and the severity and age of onset of the disease. Longer repeats cause earlier onset and more widespread neurodegeneration.

The pathogenesis of HD is still incompletely understood, but is believed to arise predominantly via a genetic gain of toxic function due to the CAG repeat expansion [9,16,17]. The polyglutamine (polyQ) expansion in the Htt protein results in change in its conformation and metabolism. The expanded protein can be cleaved into N-terminal fragments, which in most experimental systems, are more toxic that full-length Htt [18–22]. A cleavage by caspase 6 at position 586 is believed to be one of the first steps of the toxic proteolysis of Htt [23]. Transgenic mouse models expressing the caspase 6 fragment or other shorter fragments generally have more striking and robust phenotypes than transgenic mouse models expressing full-length Htt [20,24–27]. Downstream steps in the pathogenic process likely include nuclear localization and accumulation resulting in alterations of transcription, abnormal proteostasis, and interference with metabolic and mitochondrial function. These disruptions leave the cell compromised and sensitive to stress (e.g. oxidative stress) [1]. The conformational changes and aggregation of mutant Htt caused by the polyQ expansion has been extensively observed in human post-mortem brain and mouse models. These aggregates are characteristically present as nuclear inclusions [24,28], as well as aggregates elsewhere in the cell. The relationship between aggregation and cell toxicity is complex (e.g. [28–30]). Neuronal cell death in HD has some features of apoptosis with nuclear condensation and fragmentation, neurite retraction and caspase activity [11,31,32]. A recent model of inducible pluripotent cells derived from human HD patients also recapitulated many of those features [33].

Htt is a very large protein with many protein interactions, and likely with many normal functions in the cell [9,16,34–38]. There are many sites of post-translational modification, including phosphorylation, which can have substantial effects on mutant Htt cell biology, cellular localization, cleavage and cell toxicity [1,39–45]. Phosphorylation of serine 421 by Akt or SGK [46] regulates the involvement of Htt in axonal transport [47,48]. Phosphorylation of serine 421 also reduces the nuclear accumulation and cleavage of huntingtin [49], and protects against

neuronal toxicity [50–53]. Phosphorylation at positions 434, 1181 and 1201 by Cdk5 has also been reported to be protective [54,55].

The N-terminal 17 amino acids of Htt, being immediately adjacent to the polyglutamine repeat, appear to be especially important for Htt pathogenesis [56]. Phosphorylation of residues in the N-terminal 17 amino acids (threonine 3 and serines 13 and 16) can alter Htt conformation and reduce toxicity *in vitro* and *in vivo* [57–65]. Beside those few identified phosphorylation sites many other potential sites on Htt remain unknown.

As the region of the protein near the N-terminal polyglutamine repeat may be especially important for pathogenesis, we sought to determine additional sites of phosphorylation of Htt within this region. We used immunoprecipitation and mass spectrometry to identify novel phosphorylation sites within an N-terminal region fragment ending shortly before the known caspase cleavage sites. We found a number of candidate sites, and screened them for modulation of toxicity. In addition to the confirmation of known phosphorylation sites, we find that that alteration of the serine at position 116 has striking modulatory effects on Htt cell toxicity.

Materials and Methods

Antibodies and reagents

Goat polyclonal 909 antibody, prepared against the N-terminal Htt exon-1 fragment was described previously [66]; Htt monoclonal MAB5492 antibody (against residues 1–82 of Htt) was from Millipore. Actin antibody was from Sigma. Ro 31–8220 was purchased from Sigma.

Animals

For primary neurons, CD1 mice were purchased from Jackson Laboratory. This study was carried out in strict accordance with the recommendations in the Guide for the Care and Use of Laboratory Animals of the National Institutes of Health. The protocol was approved by the Johns Hopkins Animal Care and Use Committee (Protocol MO09M411).

Cell culture and transfection

Human embryonic kidney (HEK) 293FT cells were from Invitrogen. Cells were kept in DMEM (with 4.5 g/L D-Glucose, Invitrogen) supplemented with 10% FBS, 100 units/ml penicillin/streptomycin. (GIBCO), and 100 μg/ml Geneticin in 5% CO_2 at 37°C. Cells were split at a 1/10 ratio when reaching 95% confluency. For Western blot experiments, cells were plated in 6 well plates (Corning) and for mass spectrometry experiment cells were plated in 100 mm dishes (Corning). Primary mouse cortical neurons were prepared as described previously [32]. Cortices of CD1 mice at embryonic day 15.5 were dissected out, treated with trypsin (0.05% with EDTA, GIBCO) and mechanically dissociated. Neurons were suspended in Neurobasal medium supplemented with B27 (Invitrogen) and plated at 1×10^6 cell/cm^2 on poly-D-lysine coated 24 well plates (Corning). Cells were kept in Neurobasal medium supplemented with B27 and 2 mM GlutaMAX (GIBCO) in 5% CO_2 at 37°C until the day of the experiment. All cells were transfected using Lipofectamine 2000 (Invitrogen) according to the manufacturer's protocol.

Plasmids and mutagenesis

All Htt constructs used represent N-terminal fragments. They are referred to as N followed by number of amino acids present (e.g. N586). Htt expression constructs N511-52Q, N586-82Q, and N586-22Q were previously described [22]. To generate the N586 phosphorylation mutants, we used the QuikChange Site-Directed Mutagenesis Kit (Agilent) according to the manufacturer's instructions starting with 100 ng of Htt-N586-82Q DNA template and 125 ng of each primer. The sequences of primers used to generate the mutations can be found in Table S1. Primers were synthesized on an Applied Biosystem synthetizer at the Johns Hopkins University School of Medicine Synthesis and Sequencing Facility.

Purification of Htt Fragments for Mass Spectrometry

HEK 293FT cells were transfected with htt N511-52Q construct. 24 h after transfection, cells were lysed in M-PER buffer (Pierce) with protease inhibitors (Sigma) and with or without phosphatase inhibitors (Pierce, see results). The lysates were diluted 1:1 with phosphate-buffered saline (PBS) and NaCl was added to a final concentration of 150 mM. FLAG-Htt fusion proteins were immuprecipitated from 20 mg total protein using anti-FLAG M2 affinity gel (Sigma) according to the manufacturer's protocol, followed by elution with 100 μg/mL of FLAG peptide. Eluted proteins were analyzed by Western blot with a FLAG antibody (M2, Sigma). Samples were loaded on NuPAGE 4–12% BisTris polyacrylamide gel, and proteins were visualized with silver stain (SilverQuest kit, Invitrogen).

In-gel Digestion of Htt Proteins

For mass spectrometric analysis Htt containing bands were manually cut out for in-gel digestion. Gel pieces were destained with 30 mM potassium ferricyanide and 100 mM sodium thiosulfate (50:50 vol/vol), rinsed with water 3 times, incubated in 20 mM ammonium biocarbonate for 10 min, and dehydrated with acetonitrile. The process was done three times, and gel pieces were then dried in a SpeedVac. For in-gel digestion, gel pieces were incubated overnight at 37°C with 10 ng/l trypsin (Roche) in 20 mM bicarbonate. Peptides were extracted two times with 50% acetonitrile and 2% formic acid. Extracts were pooled and evaporated to dryness.

LC-MS/MS Analysis

Peptides were analyzed using QSTAR Pulsar (Applied Biosystems-MDS Sciex) interfaced with an Eksigent nano-LC system. Peptides were resuspended in 0.2% formic acid (10 μl). The solution was then separated on a 360×75 μm reverse-phase column of 10 cm of C18 beads (5 μm, 120 Å, YMC ODS-AQ, Waters) and a 10-μm emitter tip (New Objective). The gradient for high pressure liquid chromatography was 5–40% B for 25 min (A, 0.1% formic acid; B, 90% acetonitrile in 0.1% formic acid) at a 300 μL/min flow rate. Survey scans were acquired from m/z 350–1200 with up to three precursors selected for MS/MS using a dynamic exclusion of 30 s. Rolling collision energy was used to promote fragmentation. The electrospray voltage was 900 V and MS/MS spectra of ion 416.7 m/z were acquired for 3 min. The MS/MS spectra were searched against NCLInr database, using Mascot Daemon as an interface and our in-house Mascot server.

Western blotting

For Western blotting analysis, HEK 293FT cells were lysed 48 h after transfection in M-PER buffer (Pierce) with a protease inhibitors cocktail (Sigma). Protein concentrations were determined using BCA method (Bio-Rad). Proteins were separated on NuPAGE 4–12% BisTris polyacrylamide gels (Invitrogen) and transferred to nitrocellulose membranes (Bio-Rad). After 1 h blocking (PBS, 0.1% Tween 20, 5% fat free dry milk), membranes were probed with primary antibodies, washed, and incubated with peroxidase-conjugated secondary antibodies (Amersham). The signal was detected using chemi-luminescence (ECL-Plus detection

reagent, Amersham). Protein bands were quantified using Molecular Imager Gel Doc XR System and Quantity One software (Bio-Rad).

Cell death assay

To measure the survival of a small population of transfected primary neurons in culture, we established an analysis based on the nuclear condensation observed during cell death. This assay measures the Hoechst staining intensity of transfected neurons. Neurons were co-transfected at DIV5 with the Htt N586-82Q phospho-mutations and eGFP (10:1 ratio) using Lipofectamine 2000 (Invitrogen) according to the manufacturer's recommendations. After 48 h of expression, cells were fixed with 4% paraformaldehyde for 30 mn and stained with MAB5492 (Htt1-82) antibody according to the laboratory protocol. Nuclei were stained with Hoechst 33258 (bis-benzimide, Sigma-Aldritch). Image acquisition was done using the Axiovision imaging software on an Axiovert 100 inverted microscope (Carl Zeiss) using the automated Mozaix function to cover the integral surface of the wells. Analysis and quantification were performed using the Volocity software (Perkin-Elmer). In order to measure only the intensity of the nuclei of transfected cells, first specific signal of transfected Htt was isolated. Nuclei were subsequently detected in these specific regions corresponding to the transfected cells and their average intensity measured. The percentage of surviving cells was calculated as the percentage of cells for which the average intensity of nuclear staining does not exceed 200% of the average intensity of healthy untransfected nuclei. Results are shown as a percentage of survival of transfected cells, and each independent experiment represent the average of 4 wells per condition.

Time-lapse imaging

Primary neurons were co-transfected using Lipofectamine 2000 in the same conditions as described above. 38 h post-transfection, plates were transferred into the incubation chamber of an Axiovert 100 inverted microscope (Carl Zeiss) and healthy neurons expressing GFP were randomly selected and followed for 10 h with a picture taken every 10 min. 37°C and 5% CO_2 were maintained in the chamber throughout the experiment. Morphology of every neuron was quantified blindly using Axiovision software. Cells were given a value for every frame of the experiment: 100 when healthy and 0 when dead. Cells were considered dead when most of the neurites were detached from the soma and fragmented, or when the soma became totally round. Results are expressed as mean ± sem. n = 200 cells analyzed in 5 independent experiments.

Immunostaining

Cells were fixed directly in the cell culture dishes with PBS containing 4% paraformaldehyde for 30 min. After washing three times with PBS, cells were permeabilized with PBS containing 0.2% Triton X-100 for 10 minutes, then treated with blocking buffer containing 0.2% Triton X-100 and 10% goat serum for 2 h. MAB5492 antibody (1:1500) was incubated overnight at 4°C in PBS containing 10% goat serum. Cells were rinsed in PBS and incubated for 2 h with anti-mouse CY3-conjugated antibody (1:200, Jackson). Nuclei were stained with Hoechst 33342 and, after washing twice in PBS, cells were mounted onto slides using Vectashield. Confocal microscopy was performed using a Zeiss Axiovert 200 inverted microscope with 510-Meta confocal module and 63× objective.

Results

In order to identify novel phosphorylation sites in a region of Htt using mass spectrometry, we chose a fragment of 511 amino acids for study. It is slightly smaller than potential fragments generated by cleavage at the several known caspase sites, and thus is unlikely to be cleaved further by caspases in the cell during the experiment. The construct used contained an N-terminal Flag tag (Figure 1A) and a glutamine repeat length of 52. This is within the expanded range and has toxicity in cells, but does not rapidly cause aggregation in our cell system, which might interfere with immunoprecipitation.

HEK293 cells were transfected with the Htt N511-52Q construct (Figure 1A) and either stimulated with serum and lysed in the presence of phosphatase inhibitors to preserve phosphorylation events, or treated with phosphatase to eliminate any phosphorylation. Htt was purified by immunoprecipitation using antibodies to the Flag tag. The bands containing Htt were identified by Coomassie, and confirmed by Western blot. The phosphatase treatment caused a shift in migration of the expanded Htt protein suggestive of the possibility of alteration by phosphorylation (Figure 1B). Gel slices containing Htt bands were cut out from the gel and processed for mass spectrometry. In some experiments Htt tryptic peptides were enriched for phosphopeptides using a titanium dioxide column. We have obtained around 73% coverage of Htt sequence (Figure 1C) within the region excluding the polyQ and proline repeat region (which does not contain amino acids that would be susceptible to trypsin cleavage). Table 1 shows phosphorylated peptides identified in this experiment. All phosphorylation sites detected were considered for further analysis, even if they had low ion scores, so that we would avoid missing potentially important functional sites. Examples of mass spectra and the fragmentation table of the peptide containing phosphorylated S116 are presented in Figure 1D and 1E.

In order to screen for the potential functional relevance of the detected phosphorylation sites in Htt, we performed site directed mutagenesis to alter all of the sites. Figure 2A shows the sites subjected to site directed mutagenesis. In addition to the sites we identified by mass spectrometry, we also added phosphorylation sites that have been previously described as well as several additional sites in the critical N-terminal region of Htt. For each site, alterations to alanine, which would prevent phosphorylation, and to aspartate, which may mimic phosphorylation, were made. In all cases, at least two clones were generated and tested for expression to confirm that the site directed alterations did not change expression levels.

For our primary functional assay we chose expanded Htt cell toxicity, since this is a highly relevant cell phenotype for this neurodegenerative disease [67]. Our screen for toxicity was done in primary neurons. We chose N586 to do the toxicity experiments since that may be the physiologic fragment *in vivo* [23]. We chose a polyQ repeat length of 82 rather than 52 in order to achieve more robust toxicity, so that we would be able to detect potential reductions of toxicity. Since Htt can cause also cortical cell death and the cortex is affected in HD, we chose to study the toxicity on cortical neurons for their relative abundance. Since it is difficult to do Western blots from transfected cortical neurons, we measured the effect of the site directed alterations in Htt on its expression level by immunofluorescence and quantification of the intensity of fluorescent labeling. Expression level analysis was done at 48 hours, the same time point at which toxicity was measured. The levels of expression of all Htt constructs with alterations in primary cortical neurons were very comparable. Some examples are shown in Figure 2B and 2C. An additional assay to confirm

A

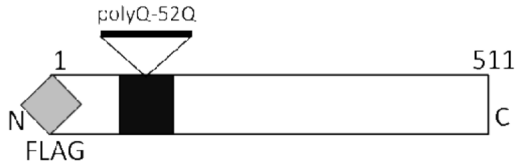

B

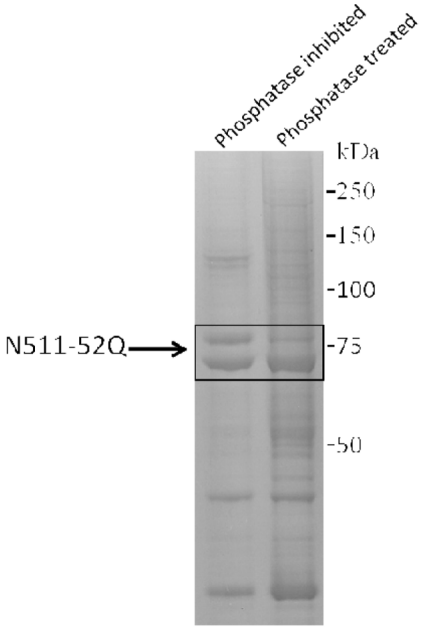

C

```
  1 MATLEKLMKAFESLKSFQQQQQQQQQQQQQQQQQQQQQQQPPPPPPPPPP
 51 PQLPQPPPQAQPLLPQPQPPPPPPPPPPGPAVAEEPLHRPKKELSATKKD
101 RVNHCLTICENIVAQSVRNSPEFQKLLGIAMELFLLCSDDAESDVRMVAD
151 ECLNKVIKALMDSNLPRLQLELYKEIKKNGAPRSLRAALWRFAELAHLVR
201 PQKCRPYLVNLLPCLTRTSKRPEESVQETLAAAVPKIMASFGNFANDNEI
251 KVLLKAFIANLKSSSPTIRRTAAGSAVSICQHSRRTQYFYSWLLNVLLGL
301 LVPVEDEHSTLLILGVLLTLRYLVPLLQQQVKDTSLKGSFGVTRKEMEVS
351 PSAEQLVQVYELTLHHTQHQDHNVVTGALELLQQLFRTPPPELLQTLTAV
401 GGIGQLTAAKEESGGRSRSGSIVELIAGGGSSCSPVLSRKQKGKVLLGEE
451 EALEDDSESRSDVSSSALTASVKDEISGELAASSGVSTPGSAGHDIITEQ
501 PRSQHTLQADS
```

D

#	b	b^{++}	b*	b*$^{++}$	b^{0}	b^{0++}	Seq.	y	y^{++}	y*	y*$^{++}$	y^{0}	y^{0++}	#
1	100.0757	50.5415					V							24
2	214.1186	107.5629	197.0921	99.0497			N	2722.3188	1361.6630	2705.2923	1353.1498	2704.3082	1352.6578	23
3	351.1775	176.0924	334.1510	167.5791			H	2608.2759	1304.6416	2591.2493	1296.1283	2590.2653	1295.6363	22
4	511.2082	256.1077	494.1816	247.5945			C	2471.2170	1236.1121	2454.1904	1227.5988	2453.2064	1227.1068	21
5	624.2922	312.6498	607.2657	304.1365			L	2311.1863	1156.0968	2294.1598	1147.5835	2293.1758	1147.0915	20
6	725.3399	363.1736	708.3134	354.6603	707.3294	354.1683	T	2198.1023	1099.5548	2181.0757	1091.0415	2180.0917	1090.5495	19
7	838.4240	419.7156	821.3974	411.2024	820.4134	410.7104	I	2097.0546	1049.0309	2080.0280	1040.5177	2079.0440	1040.0256	18
8	998.4546	499.7310	981.4281	491.2177	980.4441	490.7257	C	1983.9705	992.4889	1966.9440	983.9756	1965.9599	983.4836	17
9	1127.4972	564.2523	1110.4707	555.7390	1109.4867	555.2470	E	1823.9399	912.4736	1806.9133	903.9603	1805.9293	903.4683	16
10	1241.5402	621.2737	1224.5136	612.7604	1223.5296	612.2684	N	1694.8973	847.9523	1677.8707	839.4390	1676.8867	838.9470	15
11	1354.6242	677.8158	1337.5977	669.3025	1336.6137	668.8105	I	1580.8543	790.9308	1563.8278	782.4175	1562.8438	781.9255	14
12	1453.6926	727.3500	1436.6661	718.8367	1435.6821	718.3447	V	1467.7703	734.3888	1450.7437	725.8755	1449.7597	725.3835	13
13	1524.7298	762.8685	1507.7032	754.3552	1506.7192	753.8632	A	1368.7019	684.8546	1351.6753	676.3413	1350.6913	675.8493	12
14	1652.7883	826.8978	1635.7618	818.3845	1634.7778	817.8925	Q	1297.6647	649.3360	1280.6382	640.8227	1279.6542	640.3307	11
15	1721.8098	861.4085	1704.7832	852.8953	1703.7992	852.4033	S	1169.6062	585.3067	1152.5796	576.7934	1151.5956	576.3014	10
16	1834.8939	917.9506	1817.8673	909.4373	1816.8833	908.9453	L	1100.5847	550.7960	1083.5582	542.2827	1082.5741	541.7907	9
17	1990.9950	996.0011	1973.9684	987.4878	1972.9844	986.9958	R	987.5006	494.2540	970.4741	485.7407	969.4901	485.2487	8
18	2105.0379	1053.0226	2088.0113	1044.5093	2087.0273	1044.0173	N	831.3995	416.2034	814.3730	407.6901	813.3890	407.1981	7
19	2174.0593	1087.5333	2157.0328	1079.0200	2156.0488	1078.5280	S	717.3566	359.1819	700.3301	350.6687	699.3460	350.1767	6
20	2271.1121	1136.0597	2254.0856	1127.5464	2253.1015	1127.0544	P	648.3352	324.6712	631.3086	316.1579	630.3246	315.6659	5
21	2400.1547	1200.5810	2383.1282	1192.0677	2382.1441	1191.5757	E	551.2824	276.1448	534.2558	267.6316	533.2718	267.1396	4
22	2547.2231	1274.1152	2530.1966	1265.6019	2529.2126	1265.1099	F	422.2398	211.6235	405.2132	203.1103			3
23	2675.2817	1338.1445	2658.2551	1329.6312	2657.2711	1329.1392	Q	275.1714	138.0893	258.1448	129.5761			2
24							K	147.1128	74.0600	130.0863	65.5468			1

E

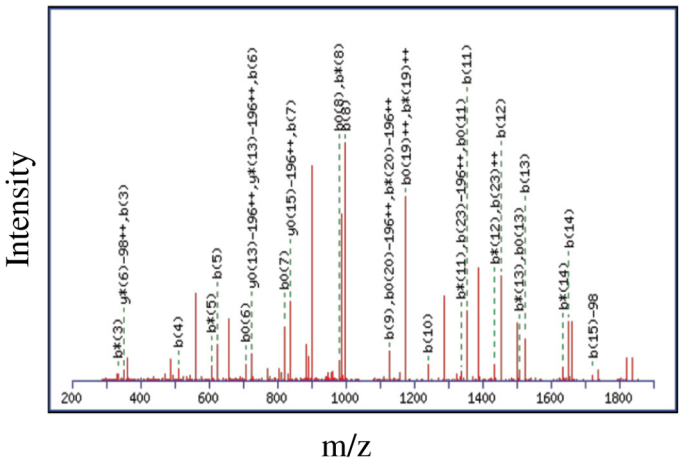

Figure 1. Isolation of Huntingtin N511 for mass spectrometry. (A) Representation of the Htt N511 construct used for transfection. (B) HEK293 cells were transfected with the N511 construct for 24 hours. Protein extracts were immunoprecipitated using Flag antibody and treated with phosphatase inhibitors or phosphatase and separated on a gel. Coomassie Blue detection of proteins in gel shows N511 overexpression. The image shown is representative of 3 replicate experiments. (C) Peptide coverage in two mass spectrometry experiments obtained from trypsin digest of Htt N511. Underlined residues indicate detection, blue indicates previously known phosphorylatable residues, red indicates novel detected sites. (D–E) Examples of mass spectra of peptide showing isotopic distribution for the site at serine 116.
doi:10.1371/journal.pone.0088284.g001

that the constructs did not alter levels of expression was done by transient transfection and Western blot analysis in HEK293 cells (Figure 2D). In our system the expression levels of the N586 fragments with 22Q or 82Q were similar as well.

The results of the screen for Htt toxicity are shown in Figure 3. We used a nuclear condensation assay which correlates well with neuronal cell death induced by Htt [32]. We observed robust cell death induced by Htt N586-82Q compared to baseline cell toxicity observed for Htt N586-22Q. As had been previously demonstrated, the change of serine 421 to aspartate caused reduced Htt toxicity, however we also observed a reduced toxicity of Htt with an alteration to an alanine at position 421. Because previous studies had shown that serine 13 and serine 16 tend to be phosphorylated in tandem, we also have included a double mutant of S13D/S16D. This construct showed significantly reduced cell toxicity. None of the other novel candidate sites that we identified showed significant effect on expanded Htt cell toxicity, except for serine 116. Strikingly, change of serine 116 to alanine in Htt results in significantly decreased cell toxicity in the nuclear condensation assay. By contrast, change to aspartate had no significant effect.

In order to confirm the effect of the alterations of phosphorylation sites in expanded Htt on its toxicity and to demonstrate directly that these alterations affected Htt-mediated neuronal cell death in culture, we used a time lapse video microscopy assay. This method is comparable to a time lapse analysis method used in the Finkbeiner laboratory [68], [69], but is set up to be useable with standard microscopy facilities without custom software or robotics. The assay makes it possible to follow cells over time by video microscopy, in this case beginning at hour 38 and ending at hour 48 post-transfection, which is the same time point at which cell toxicity is measured using the nuclear condensation assay. At the beginning of the experiment, cells are still showing healthy morphology and deteriorate over time. The time frame of degeneration is consistent with the nuclear condensation assay which shows significant death only after 36 hours [32]. As shown in Figure 4A, this assay demonstrated robust neuronal cell death in neurons transfected with Htt-N586-82Q compared to neurons transfected with normal Htt or GFP alone. We observed a significant reduction in toxicity of Htt-N586-82Q S116A, closely paralleling the results in the initial screen using the nuclear condensation cell death assay (Figure 4B). As in the nuclear condensation assay, the phosphomimetic alteration S116D did not cause a dramatically change in Htt toxicity though there is a suggestion that there may be an increase in toxicity. In the time lapse assay the alteration at position 421 did not have a dramatic effect, but had a trend toward decreasing toxicity.

Table 1. Identified phosphorylarion peptides.

Phosphorylated Peptide	Residue	Mascot Score
R.VNHCLTICENIVAQSVRNSPEFQK.L	S116, S120	62
R.TAAGSAVSICQHSR.R	T271	78
R.SRSGSIVELIAGGGSSCSPVLSR.K	S417	70
R.SRSGSIVELIAGGGSSCSPVLSR.K	S421, S431	64
R.SGSIVELIAGGGSSCSPVLSR.K	S421, S434	87
K.VLLGEEEALEDDSESRSDVSSSALTASVK.D	S457	72
K.VLLGEEEALEDDSESRSDVSSSALTASVK.D	S459	92
K.VLLGEEEALEDDSESRSDVSSSALTASVK.D	S461	99
R.SDVSSSALTASVK.D	S464	57
K.VLLGEEEALEDDSESRSDVSSSALTASVK.D	S465, S466	59
K.DEISGELAASSGVSTPGSAGHDIITEQPR.S	S487, T488	70
K.DEISGELAASSGVSTPGSAGHDIITEQPR.S	S491	104

doi:10.1371/journal.pone.0088284.t001

Discussion

In this study we have used mass spectrometry to identify potential phosphorylation sites within the N-terminal region of Htt. We have identified novel potential sites, and have confirmed previously known S421 phosphorylation site. Using a nuclear condensation cell toxicity assay in primary neurons, we set up a screen to evaluate the effects of alterations of phoshorylation sites in polyQ-expanded Htt on its toxicity. Alanine replacement at one site, serine 116, caused a significant decrease of Htt-mediated cell toxicity. We confirmed this effect using a cell death assay based on time lapse video microscopy to directly track cell death.

Strengths of this study include the identification of several novel candidate phosphorylation sites, focusing on the N-terminus of Htt near the polyQ repeat, a region of the protein likely to be relevant for HD pathogenesis. We were able to determine a functional effect of an alteration of at least one of these sites.

There were several limitations of the study. The discovery experiments were all carried out *in vitro*, and relied on overexpression in non-neuronal cell lines. We did not completely cover the N-terminal 511 amino acids of Htt, though we did achieve 73.14% coverage of the region (excluding the previously studied N-terminal 17 amino acids, the polyQ repeat and the proline repeats, which do not contain any residues which could be phosphorylated). A number of the phosphorylation sites we found did not have high ion scores, however our goal was to be inclusive rather than exclusive in pursuing candidate sites, and then to use functional assays to identify sites with potential physiologic relevance.

We have included the phosphorylation sites within the N-terminal 17 amino acid region in the functional studies because of the previous reports of protective effects of Htt phosphorylation within this region. Although, because of the unfavorable configuration of tryptic cleavage sites in this region, we did not identify Htt phosphorylation sites within its N-terminus. Similar to previous studies, we found that phospho-mimetic alteration at the S13/16 sites ameliorated toxicity.

We also studied the previously reported phosphorylation at S421 and confirmed the neuroprotection [50] with replacement by aspartate. Unlike one previous study, however, we did not find that substitution of S421 by alanine had no effect. By contrast we found suggestion of some protection. The reason for this discrepancy is not clear at the moment. Phosphorylation of Htt at S421 by Akt and SGK kinases has been reported to reduce Htt

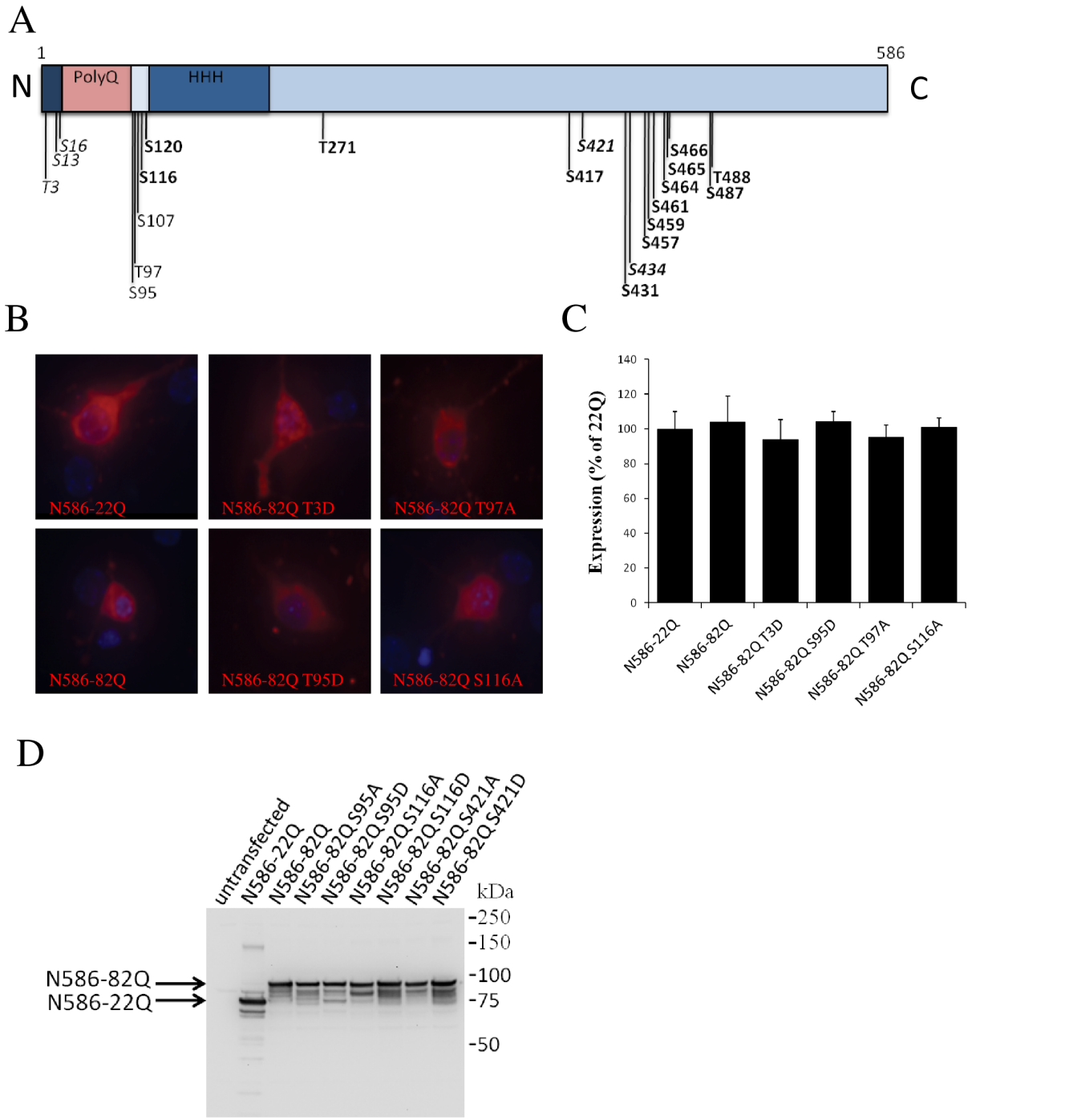

Figure 2. Generation and expression of N586-82Q constructs with phospho-site alterations. (A) Schematic representation of the Htt N586 and the sites altered. Italics indicate previously described phosphorylation sites. Detected sites are in bold. (B) Expression of constructs in primary cortical neurons. (C) Quantification of expression of N586 constructs in primary neurons. Fluorescence was quantified using Volocity, and results are expressed as percent of N586-22Q level of expression. (D) Western blot of expression of N586 constructs with phospho-site alterations in primary cortical neurons. The image shown is representative of 4 replicate experiments.
doi:10.1371/journal.pone.0088284.g002

toxicity, and to restore axonal transport in neurons [47,50]. Our results, demonstrating that alteration preventing phosphorylation of S421 reduce Htt neuronal toxicity seems to contradict this notion. This raises a possibility that S421D mutation may not mimic phosphorylation, and that both alterations prevent phosphorylation of S421, which turns out to reduce Htt toxicity, at least in our system. We wonder if the previous experiments with Akt and SGK kinases might have found neuroprotection due to other effects of the kinases besides direct effects on Htt itself. Certainly Akt is well known to be part of signaling pathways promoting global cellular survival.

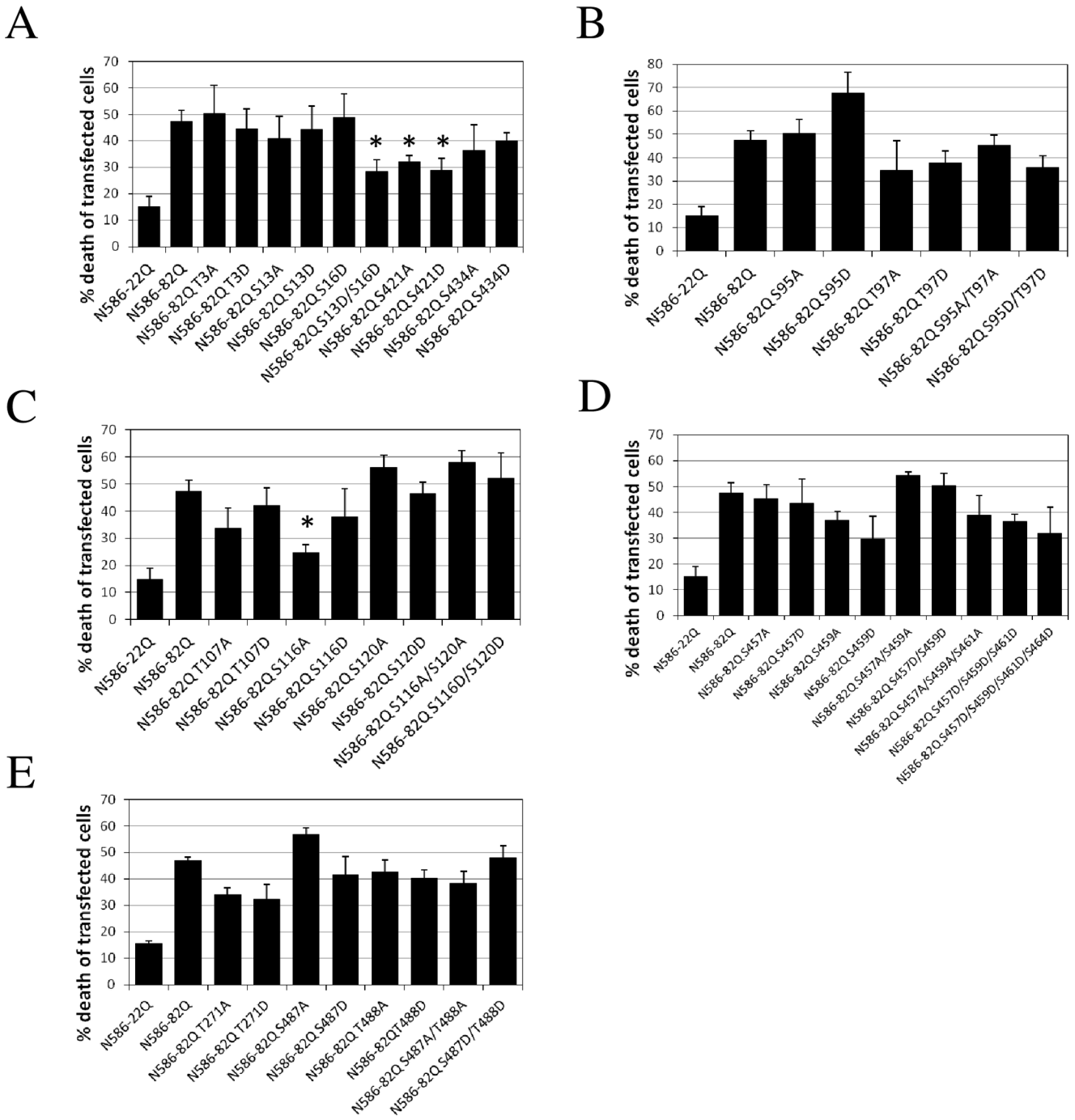

Figure 3. Cell toxicity of N586-82Q constructs with alterations of phospho-sites in primary neurons. Primary cortical neurons were transfected at DIV5. Automated quantification of nuclear condensation was performed 48 hours after transfection using Volocity software. (A) Toxicity of constructs with alterations of previously identified Htt phosphorylation sites. (B) Toxicity of constructs with alterations of putative Htt phosphorylation sites located between position 1 and 100. (C) Toxicity of constructs with alterations of putative Htt phosphorylation sites located between 100 and 200. (D) Toxicity of constructs with alterations of putative Htt phosphorylation sites located at the 457–464 cluster. (E) Toxicity of constructs with alterations of putative Htt phosphorylation sites located between 200 and 586. Results are expressed as mean ± sem. n = 5 independent experiments per condition. * $p<0.05$ compared to N586-82Q.
doi:10.1371/journal.pone.0088284.g003

Neuronal cell death is highly relevant to pathogenesis of HD, and cell loss in postmortem HD striatum best reflects premortem motor impairment and functional disability [67]. This assay has the disadvantage of being relatively low throughput, but feasible for the relatively small number of sites we had to study. The only alteration which significantly altered expanded Htt toxicity was S116A; however some of the other alterations, such as T107A and the cluster at 457/459/461/464 showed trends, and might be followed up in future studies.

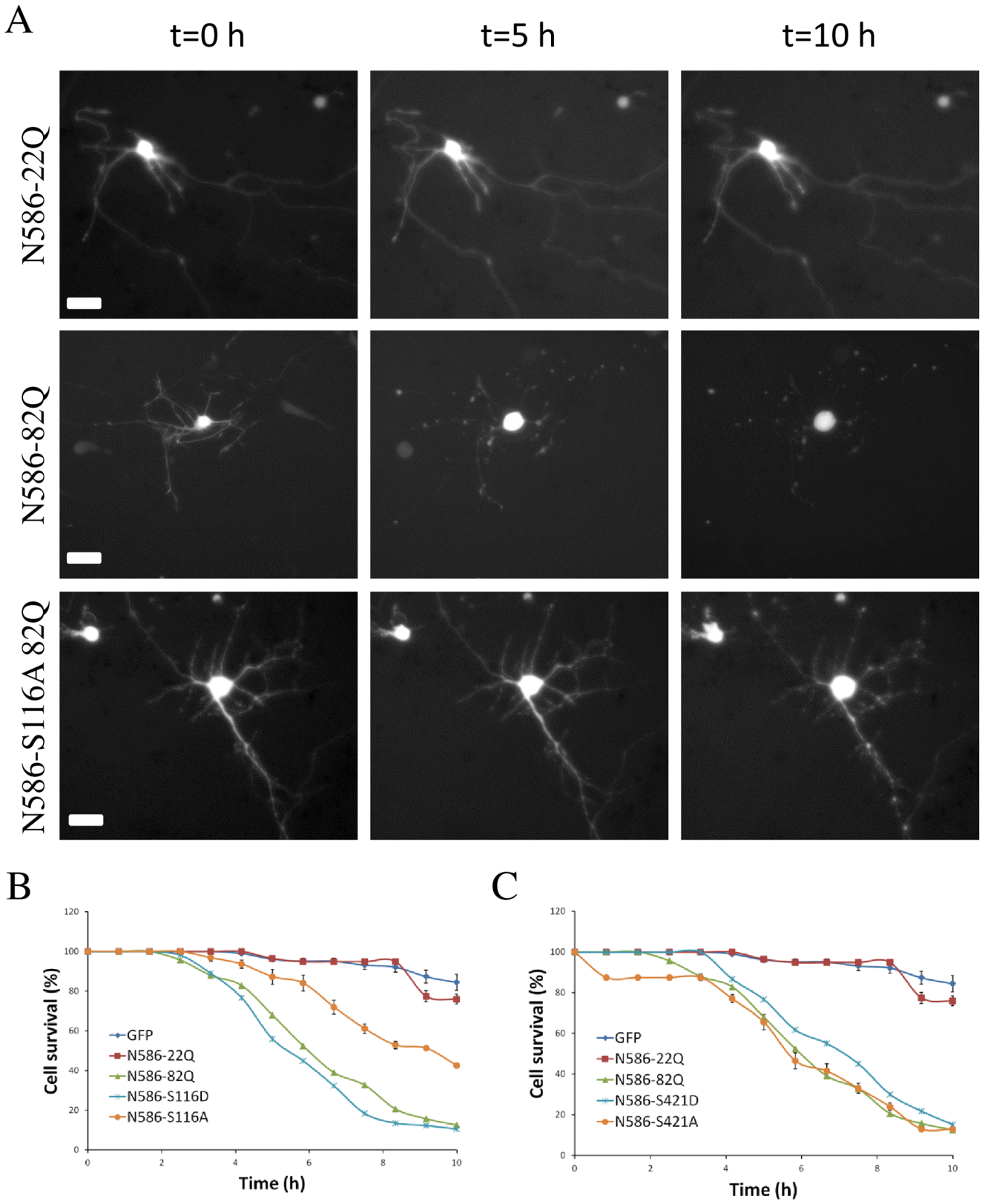

Figure 4. Time lapse imaging of toxicity of N586 constructs. Primary cortical neurons were co-transfected at DIV5. Beginning 24 hours after transfection, GFP positive neurons were imaged every 10 mn for 10 hours. (A) Representative images of cells transfected with N586-22Q (top row), N586-82Q (middle row), or N586-82Q S116A (bottom row) at t = 0 (left column), t = 5 h (center column), and t = 10 h (right column). (B) Quantification of cell survival. For each time point cells were given the value of 100 if alive and 0 if dead. Results are expressed as mean ± sem. n = 200 cells analyzed in 5 independent experiments.
doi:10.1371/journal.pone.0088284.g004

The S116A alteration showed significant and reproducible protection in the nuclear condensation assay. This was clearly supported by the data from the time-lapse microscopy data, which showed substantial decrease of Htt-mediated cell death. It should be kept in mind that cell culture experiments with over-expressed protein involve an *in vitro* short-duration system, and will need *in vivo* confirmation. In our experiments, we saw protection with the serine to alanine alteration, but no change with the serine to aspartate alteration. This could indicate that the stoichiometry of phosphorylation at this site is relatively high or possibly that the aspartate substitution does not well mimic the effects of phosphoserine at this site.

In this study we have attempted to find phosphorylation sites with functional relevance that could be involved in disease pathogenesis. We found a striking effect of alteration of the S116 site on mutant Htt cellular toxicity. This raises the possibility that phosphorylation of S116 could be involved in HD pathogenesis. This would be reminiscent of other neurodegenerative diseases in which phosphorylation is known to modulate cellular toxicity of the relevant disease protein. For instance, in the case of SCA1, alteration of serine 776 in a transgenic mouse model substantially ameliorated the phenotype [70]. Phosphorylation of tau is involved in Alzheimer's disease and other taupathies, and is likely to have an important role in promoting AD pathogenesis [71]. Phosphorylation of α-synuclein at S129 has been implicated in PD pathogenesis [72].

Htt phosphorylation has been suggested to have potential therapeutic relevance. Small molecule modulation of phosphorylation within the first 17 amino acids alters Htt sub-cellular localization and Htt cleavage and toxicity [58]. Inhibition of calcineurin by FK506 also can have a protective role through increase of Htt phosphorylation at serine 421 [51], though targeting the m-TOR pathway with Everolimus did not have a similar effect [73]. Ganglioside GM1 induces phosphorylation of mutant Htt and ameliorates the abnormal phenotype in HD mice [63]. Thus, a better understanding of phosphorylation of Htt may provide therapeutic targets for treatment of HD.

The candidate phosphorylation sites identified here still need to be confirmed *in vivo*. However, if phosphorylation of Htt at serine 116 can be shown to be relevant *in vivo*, then we would propose that phosphorylation of S116 has an important modulatory role in HD pathogenesis. Because changing the serine to alanine is protective, inhibiting the kinase or kinases that phosphorylate this site should also be protective. Thus this phosphorylation event could be a candidate therapeutic target for HD.

Supporting Information

Table S1 Primer sequences for Htt-N586-82Q site directed mutagenesis.
(DOCX)

Author Contributions

Conceived and designed the experiments: EEW NA RO TR RNC CAR. Performed the experiments: EEW NA EWR RO. Analyzed the data: EEW NA EWR RO TR CAR. Contributed reagents/materials/analysis tools: EWR RO RNC CAR. Wrote the paper: EEW NA TR CAR.

References

1. Ross CA, Tabrizi SJ (2011) Huntington's disease: from molecular pathogenesis to clinical treatment. Lancet Neurol 10: 83–98.
2. Gusella JF, MacDonald ME (2006) Huntington's disease: seeing the pathogenic process through a genetic lens. Trends Biochem Sci 31: 533–540.
3. MacDonald ME (2003) Huntingtin: alive and well and working in middle management. Sci STKE 2003: pe48.
4. Walker FO (2007) Huntington's Disease. Semin Neurol 27: 143–150.
5. Imarisio S, Carmichael J, Korolchuk V, Chen CW, Saiki S, et al. (2008) Huntington's disease: from pathology and genetics to potential therapies. Biochem J 412: 191–209.
6. Krobitsch S, Kazantsev AG (2011) Huntington's disease: From molecular basis to therapeutic advances. Int J Biochem Cell Biol 43: 20–24.
7. Shang H, Danek A, Landwehrmeyer B, Burgunder JM (2012) Huntington's disease: new aspects on phenotype and genotype. Parkinsonism Relat Disord 18 Suppl 1: S107–109.
8. Finkbeiner S (2011) Huntington's Disease. Cold Spring Harb Perspect Biol 3.
9. Zuccato C, Valenza M, Cattaneo E (2005) Molecular mechanisms and potential therapeutical targets in Huntington's disease. Physiol Rev 90: 905–981.
10. Ross CA, Shoulson I (2009) Huntington disease: pathogenesis, biomarkers, and approaches to experimental therapeutics. Parkinsonism Relat Disord 15 Suppl 3: S135–138.
11. Cowan CM, Raymond LA (2006) Selective neuronal degeneration in Huntington's disease. Curr Top Dev Biol 75: 25–71.
12. Reiner A, Dragatsis I, Dietrich P (2011) Genetics and neuropathology of Huntington's disease. Int Rev Neurobiol 98: 325–372.
13. Vonsattel JP, Keller C, Cortes Ramirez EP (2011) Huntington's disease - neuropathology. Handb Clin Neurol 100: 83–100.
14. Ehrlich ME (2012) Huntington's disease and the striatal medium spiny neuron: cell-autonomous and non-cell-autonomous mechanisms of disease. Neurotherapeutics 9: 270–284.
15. The Huntington's Disease Collaborative Research Group (1993) A novel gene containing a trinucleotide repeat that is expanded and unstable on Huntington's disease chromosomes. The Huntington's Disease Collaborative Research Group. Cell 72: 971–983.
16. Borrell-Pages M, Zala D, Humbert S, Saudou F (2006) Huntington's disease: from huntingtin function and dysfunction to therapeutic strategies. Cell Mol Life Sci 63: 2642–2660.
17. Zheng L, Diamond JM, Denton DL (2013) Evaluation of whole effluent toxicity data characteristics and use of Welch's T-test in the test of significant toxicity analysis. Environ Toxicol Chem 32: 468–474.
18. DiFiglia M, Sapp E, Chase KO, Davies SW, Bates GP, et al. (1997) Aggregation of huntingtin in neuronal intranuclear inclusions and dystrophic neurites in brain. Science 277: 1990–1993.
19. Qin ZH, Gu ZL (2004) Huntingtin processing in pathogenesis of Huntington disease. Acta Pharmacol Sin 25: 1243–1249.
20. Waldron-Roby E, Ratovitski T, Wang X, Jiang M, Watkin E, et al. (2012) Transgenic mouse model expressing the caspase 6 fragment of mutant huntingtin. J Neurosci 32: 183–193.
21. Ratovitski T, Nakamura M, D'Ambola J, Chighladze E, Liang Y, et al. (2007) N-terminal proteolysis of full-length mutant huntingtin in an inducible PC12 cell model of Huntington's disease. Cell Cycle 6: 2970–2981.
22. Ratovitski T, Gucek M, Jiang H, Chighladze E, Waldron E, et al. (2009) Mutant huntingtin N-terminal fragments of specific size mediate aggregation and toxicity in neuronal cells. J Biol Chem 284: 10855–10867.
23. Graham RK, Deng Y, Slow EJ, Haigh B, Bissada N, et al. (2006) Cleavage at the caspase-6 site is required for neuronal dysfunction and degeneration due to mutant huntingtin. Cell 125: 1179–1191.
24. Davies SW, Turmaine M, Cozens BA, DiFiglia M, Sharp AH, et al. (1997) Formation of neuronal intranuclear inclusions underlies the neurological dysfunction in mice transgenic for the HD mutation. Cell 90: 537–548.
25. Schilling G, Becher MW, Sharp AH, Jinnah HA, Duan K, et al. (1999) Intranuclear inclusions and neuritic aggregates in transgenic mice expressing a mutant N-terminal fragment of huntingtin. Hum Mol Genet 8: 397–407.
26. Crook ZR, Housman D (2011) Huntington's disease: can mice lead the way to treatment? Neuron 69: 423–435.
27. Heng MY, Detloff PJ, Albin RL (2008) Rodent genetic models of Huntington disease. Neurobiol Dis 32: 1–9.
28. Arrasate M, Finkbeiner S (2012) Protein aggregates in Huntington's disease. Exp Neurol 238: 1–11.
29. Ross CA, Poirier MA (2004) Protein aggregation and neurodegenerative disease. Nature Med 10: S10–S17.
30. Poirier MA, Jiang H, Ross CA (2005) A structure-based analysis of huntingtin mutant polyglutamine aggregation and toxicity: evidence for a compact beta-sheet structure. Hum Mol Genet 14: 765–774.
31. Bossy-Wetzel E, Petrilli A, Knott AB (2008) Mutant huntingtin and mitochondrial dysfunction. Trends Neurosci 31: 609–616.
32. Nucifora LG, Burke KA, Feng X, Arbez N, Zhu S, et al. (2012) Identification of novel potentially toxic oligomers formed in vitro from mammalian-derived expanded huntingtin exon-1 protein. J Biol Chem 287: 16017–16028.
33. The HD iPsc Consortium (2012) Induced Pluripotent Stem Cells from Patients with Huntington's Disease Show CAG-Repeat-Expansion-Associated Phenotypes. Cell Stem Cell 11: 264–278.

34. Cattaneo E, Zuccato C, Tartari M (2005) Normal huntingtin function: an alternative approach to Huntington's disease. Nat Rev Neurosci 6: 919–930.
35. Caviston JP, Holzbaur EL (2009) Huntingtin as an essential integrator of intracellular vesicular trafficking. Trends Cell Biol 19: 147–155.
36. Shirasaki DI, Greiner ER, Al-Ramahi I, Gray M, Boontheung P, et al. (2012) Network organization of the huntingtin proteomic interactome in mammalian brain. Neuron 75: 41–57.
37. Culver BP, Savas JN, Park SK, Choi JH, Zheng S, et al. (2012) Proteomic analysis of wild-type and mutant huntingtin-associated proteins in mouse brains identifies unique interactions and involvement in protein synthesis. J Biol Chem 287: 21599–21614.
38. Ratovitski T, Chighladze E, Arbez N, Boronina T, Herbrich S, et al. (2012) Huntingtin protein interactions altered by polyglutamine expansion as determined by quantitative proteomic analysis. Cell Cycle 11: 2006–2021.
39. Ehrnhoefer DE, Skotte NH, Savill J, Nguyen YT, Ladha S, et al. (2011) A quantitative method for the specific assessment of caspase-6 activity in cell culture. PLoS One 6: e27680.
40. Schilling B, Gafni J, Torcassi C, Cong X, Row RH, et al. (2006) Huntingtin phosphorylation sites mapped by mass spectrometry. Modulation of cleavage and toxicity. J Biol Chem 281: 23686–23697.
41. Mitsui K, Doi H, Nukina N (2006) Proteomics of polyglutamine aggregates. Methods Enzymol 412: 63–76.
42. Wang Y, Lin F, Qin ZH (2010) The role of post-translational modifications of huntingtin in the pathogenesis of Huntington's disease. Neurosci Bull 26: 153–162.
43. Young FB, Franciosi S, Spreeuw A, Deng Y, Sanders S, et al. (2012) Low levels of human HIP14 are sufficient to rescue neuropathological, behavioural, and enzymatic defects due to loss of murine HIP14 in Hip14-/- mice. PLoS One 7: e36315.
44. Dong G, Callegari E, Gloeckner CJ, Ueffing M, Wang H (2012) Mass spectrometric identification of novel posttranslational modification sites in Huntingtin. Proteomics 12: 2060–2064.
45. Cong X, Held JM, DeGiacomo F, Bonner A, Chen JM, et al. (2011) Mass spectrometric identification of novel lysine acetylation sites in huntingtin. Mol Cell Proteomics 10: M111 009829.
46. Rangone H, Poizat G, Troncoso J, Ross CA, MacDonald ME, et al. (2004) The serum- and glucocorticoid-induced kinase SGK inhibits mutant huntingtin-induced toxicity by phosphorylating serine 421 of huntingtin. Eur J Neurosci 19: 273–279.
47. Colin E, Zala D, Liot G, Rangone H, Borrell-Pages M, et al. (2008) Huntingtin phosphorylation acts as a molecular switch for anterograde/retrograde transport in neurons. EMBO J 27: 2124–2134.
48. Zala D, Colin E, Rangone H, Liot G, Humbert S, et al. (2008) Phosphorylation of mutant huntingtin at S421 restores anterograde and retrograde transport in neurons. Hum Mol Genet 17: 3837–3846.
49. Warby SC, Doty CN, Graham RK, Shively J, Singaraja RR, et al. (2009) Phosphorylation of huntingtin reduces the accumulation of its nuclear fragments. Mol Cell Neurosci 40: 121–127.
50. Humbert S, Bryson EA, Cordelieres FP, Connors NC, Datta SR, et al. (2002) The IGF-1/Akt pathway is neuroprotective in Huntington's disease and involves Huntingtin phosphorylation by Akt. Dev Cell 2: 831–837.
51. Pardo R, Colin E, Regulier E, Aebischer P, Deglon N, et al. (2006) Inhibition of calcineurin by FK506 protects against polyglutamine-huntingtin toxicity through an increase of huntingtin phosphorylation at S421. J Neurosci 26: 1635–1645.
52. Metzler M, Gan L, Mazarei G, Graham RK, Liu L, et al. (2010) Phosphorylation of huntingtin at Ser421 in YAC128 neurons is associated with protection of YAC128 neurons from NMDA-mediated excitotoxicity and is modulated by PP1 and PP2A. J Neurosci 30: 14318–14329.
53. Jablonski MR, Cooper L, Jacob DA (2011) NMDA receptor excitotoxicity: impact on phosphatase activity and phosphorylation of huntingtin. J Neurosci 31: 4357–4359.
54. Luo S, Vacher C, Davies JE, Rubinsztein DC (2005) Cdk5 phosphorylation of huntingtin reduces its cleavage by caspases: implications for mutant huntingtin toxicity. J Cell Biol 169: 647–656.
55. Anne SL, Saudou F, Humbert S (2007) Phosphorylation of huntingtin by cyclin-dependent kinase 5 is induced by DNA damage and regulates wild-type and mutant huntingtin toxicity in neurons. J Neurosci 27: 7318–7328.
56. Maiuri T, Woloshansky T, Xia J, Truant R (2012) The huntingtin N17 domain is a multifunctional CRM1 and Ran-dependent nuclear and cilial export signal. Hum Mol Genet 22: 1383–1394.
57. Khoshnan A, Patterson PH (2011) The role of IkappaB kinase complex in the neurobiology of Huntington's disease. Neurobiol Dis 43: 305–311.
58. Atwal RS, Desmond CR, Caron N, Maiuri T, Xia J, et al. (2011) Kinase inhibitors modulate huntingtin cell localization and toxicity. Nat Chem Biol 7: 453–460.
59. Greiner ER, Yang XW (2011) Huntington's disease: flipping a switch on huntingtin. Nat Chem Biol 7: 412–414.
60. Havel LS, Wang CE, Wade B, Huang B, Li S, et al. (2011) Preferential accumulation of N-terminal mutant huntingtin in the nuclei of striatal neurons is regulated by phosphorylation. Hum Mol Genet 20: 1424–1437.
61. Gu X, Greiner ER, Mishra R, Kodali R, Osmand A, et al. (2009) Serines 13 and 16 are critical determinants of full-length human mutant huntingtin induced disease pathogenesis in HD mice. Neuron 64: 828–840.
62. Aiken CT, Steffan JS, Guerrero CM, Khashwji H, Lukacsovich T, et al. (2009) Phosphorylation of threonine 3: implications for Huntingtin aggregation and neurotoxicity. J Biol Chem 284: 29427–29436.
63. Di Pardo A, Maglione V, Alpaugh M, Horkey M, Atwal RS, et al. (2012) Ganglioside GM1 induces phosphorylation of mutant huntingtin and restores normal motor behavior in Huntington disease mice. Proc Natl Acad Sci U S A 109: 3528–3533.
64. Thompson LM, Aiken CT, Kaltenbach LS, Agrawal N, Illes K, et al. (2009) IKK phosphorylates Huntingtin and targets it for degradation by the proteasome and lysosome. J Cell Biol 187: 1083–1099.
65. Mishra R, Hoop CL, Kodali R, Sahoo B, van der Wel PC, et al. (2012) Serine phosphorylation suppresses huntingtin amyloid accumulation by altering protein aggregation properties. J Mol Biol 424: 1–14.
66. Peters MF, Ross CA (2001) Isolation of a 40-kDa Huntingtin-associated protein. J Biol Chem 276: 3188–3194.
67. Guo Z, Rudow G, Pletnikova O, Codispoti KE, Orr BA, et al. (2012) Striatal neuronal loss correlates with clinical motor impairment in Huntington's disease. Mov Disord 27: 1379–1386.
68. Miller J, Arrasate M, Shaby BA, Mitra S, Masliah E, et al. (2010) Quantitative relationships between huntingtin levels, polyglutamine length, inclusion body formation, and neuronal death provide novel insight into huntington's disease molecular pathogenesis. J Neurosci 30: 10541–10550.
69. Arrasate M, Finkbeiner S (2005) Automated microscope system for determining factors that predict neuronal fate. Proc Natl Acad Sci U S A 102: 3840–3845.
70. Emamian ES, Kaytor MD, Duvick LA, Zu T, Tousey SK, et al. (2003) Serine 776 of ataxin-1 is critical for polyglutamine-induced disease in SCA1 transgenic mice. Neuron 38: 375–387.
71. Martin L, Latypova X, Wilson CM, Magnaudeix A, Perrin ML, et al. (2013) Tau protein kinases: involvement in Alzheimer's disease. Ageing Res Rev 12: 289–309.
72. Chau KY, Ching HL, Schapira AH, Cooper JM (2009) Relationship between alpha synuclein phosphorylation, proteasomal inhibition and cell death: relevance to Parkinson's disease pathogenesis. J Neurochem 110: 1005–1013.
73. Fox JH, Connor T, Chopra V, Dorsey K, Kama JA, et al. (2010) The mTOR kinase inhibitor Everolimus decreases S6 kinase phosphorylation but fails to reduce mutant huntingtin levels in brain and is not neuroprotective in the R6/2 mouse model of Huntington's disease. Mol Neurodegener 5: 26.